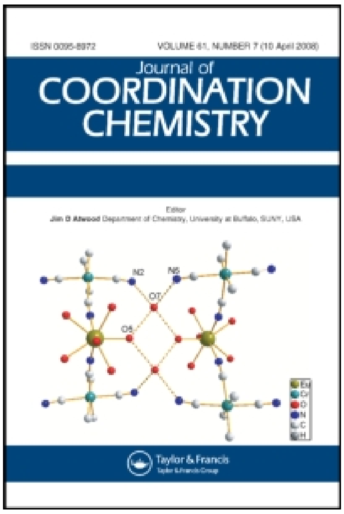

Journal of Coordination Chemistry
Publication details, including instructions for authors and subscription information:
http://www.informaworld.com/smpp/title~content=t713455674

Crystal structures and intermolecular interactions of two copper(II) complexes with an asymmetric diazine ligand

Dan Wang[a]; Shi-Xiong Liu[a]
[a] Department of Chemistry, Fuzhou University, Fuzhou, Fujian, China

To cite this Article Wang, Dan and Liu, Shi-Xiong(2009) 'Crystal structures and intermolecular interactions of two copper(II) complexes with an asymmetric diazine ligand', Journal of Coordination Chemistry, 62: 11, 1791 — 1800, First published on: 29 July 2010 (iFirst)

To link to this Article: DOI: 10.1080/00958970902718630

URL: http://dx.doi.org/10.1080/00958970902718630

Journal of Coordination Chemistry
Vol. 62, No. 11, 1 June 2009, 1791–1800

Crystal structures and intermolecular interactions of two copper(II) complexes with an asymmetric diazine ligand

DAN WANG and SHI-XIONG LIU*

Department of Chemistry, Fuzhou University, Fuzhou, Fujian, 350002, China

(*Received 26 June 2008; in final form 3 September 2008*)

Reactions of asymmetric ligand *N*-phenylacetyl picoloylhydrazide (HL) and copper(II) acetate/chloride give two complexes CuL_2 (**1**) and $Cu_2Cl_2L_2$ (**2**). The coordination geometries of Cu(II) in **1** and **2** are a severely distorted octahedron and a distorted square pyramid, respectively. The binuclear copper complex **2** contains a centrosymmetric $Cu_2(\mu\text{-}Cl)_2$ core. Individual molecules of **1** and **2** further self-assemble through non-covalent intermolecular bonds in the solid state to form extended 2-D polymers. The magnetic properties, IR, EA, and solid-state photoluminescence properties of the title complexes are presented.

Keywords: Copper(II); Crystal structure; Magnetic properties; Photoluminescence; Tridentate ligand

1. Introduction

Design and synthesis of new multidentate ligands are important and there is much interest in metal complexes with multidentate diazine (N–N) ligands due to the variety of structures and magnetic properties [1–6]. Many mono- and polynuclear complexes with multidentate ligands have been obtained. Ligands with high asymmetry may result in the highly asymmetric supramolecules [7, 8]. Non-covalent intermolecular bonds such as hydrogen bonds and $\pi \cdots \pi$ interactions play an important role in crystal engineering and in stability of metal complexes [9].

As continuation of our preparations of metal complexes with multidentate diazine ligands, we explore the assembly by new asymmetric diazine ligands. Herein, we report the syntheses, crystal structures and characterization of CuL_2 (**1**) and $Cu_2Cl_2L_2$ (**2**) with an asymmetric tridentate ligand, *N*-phenylacetyl picoloylhydrazide (HL); in **1** and **2**, HL is coordinated to Cu(II) through its pyridine nitrogen, one hydrazine nitrogen and an acyl oxygen. Binding models of L in the complexes are shown in scheme 1. Complex **1** forms a 2-D supramolecular structure through hydrogen bonds, $\pi \cdots \pi$ interactions and C–H$\cdots\pi$ interactions, while **2** is extended into 2-D supramolecular layers via only hydrogen bonds.

---

*Corresponding author. Email: shixiongliu@yahoo.com

Journal of Coordination Chemistry
ISSN 0095-8972 print/ISSN 1029-0389 online © 2009 Taylor & Francis
DOI: 10.1080/00958970902718630

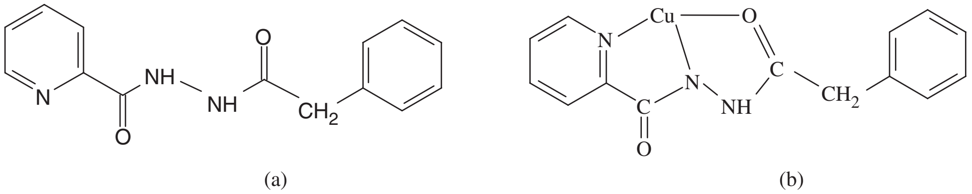

Scheme 1. Ligand HL (a) and basic binding sites of L in **1** and **2** (b).

2. Experimental

2.1. *Syntheses*

Elemental analyses of carbon, hydrogen, and nitrogen were carried out with an Elementar Vario EL III microanalyzer. The infrared spectra were recorded on a Perkin–Elmer Spectrum 2000 spectrophotometer from 4000–400 cm^{-1} using KBr pellets. Solid-state fluorescent studies were conducted at room temperature on an Edinburgh FL-FS920 TCSPC system. Variable-temperature magnetic susceptibility and field-dependent magnetization measurements on polycrystalline samples were performed on a PPMS 9T Quantum Design SQUID magnetometer. All data were corrected for diamagnetism estimated from Pascal's constants.

2.1.1. HL (*N*-phenylacetyl picoloylhydrazide). Phenylacetyl chloride (3.91 mL, 33.4 mmol) was added to a solution of phenyl acetic acid (2.73 mL, 33.4 mmol) and triethylamine (4.66 mL, 33.4 mmol) in 60 mL of chloroform at 0°C. The reaction mixture was then slowly warmed to room temperature. When picoloylhydrazide (4.238 g, 27.9 mmol) was added to the reaction mixture, a white suspension was obtained. The resulting suspension was filtered off and rinsed with chloroform and diethyl ether.

2.1.2. CuL_2 (1). Methanol solution (5 mL) of $Cu(OAc)_2 \cdot H_2O$ (0.262 g, 1 mmol) was added to a stirred CH_2Cl_2 solution (5 mL) of HL (2 mmol). After stirring for 2 h, the solution was filtered and kept for crystallization. Green crystals of **1** suitable for X-ray diffraction were obtained after 2 weeks. Yield: 62% (based on copper). Anal. Calcd for $Cu(C_{14}H_{12}N_3O_2)_2$: C, 58.79; H, 4.23; N, 14.69%. Found: C, 58.57; H, 4.16; N, 14.65%.

2.1.3. $Cu_2Cl_2L_2$ (2). To HL (1 mmol) in CH_2Cl_2 (5 mL) was added an equal molar amount of $CuCl_2 \cdot 2H_2O$ in methanol (5 mL). The green solution was stirred at room temperature for 30 min, filtered, and allowed to stand at room temperature for 3 weeks. Green crystals of **2** suitable for X-ray diffraction were formed. Yield: 65% (based on copper). Anal. Calcd for $Cu_2(C_{14}H_{12}N_3O_2)_2Cl_2$: C, 47.60; H, 3.42; N, 11.89%. Found: C, 47.56; H, 3.31; N, 11.67%.

2.2. *X-ray crystallography*

Crystals of the title complexes were mounted on glass fibers. Intensity data were collected at a Rigaku RAPID Weissengberg IP diffractometer with

Table 1. Crystal data and structural refinement parameters for **1** and **2**.

Compounds	**1**	**2**
Formula	$CuC_{28}H_{24}N_6O_4$	$Cu_2C_{28}H_{24}$ $N_6O_4Cl_2$
Formula weight	572.07	706.51
Crystal size (mm)	0.18 0.14 0.12	0.25 0.15 0.10
Crystal system	Orthorhombic	Monoclinic
Space group	$Pna2_1$	$P2_1/c$
Unit cell dimensions (Å, °)		
a	9.3846(19)	6.082(2)
b	18.479(4)	10.065(4)
c	15.232(3)	23.851(10)
β	90	97.98(2)
V (Å^3)	2641.6(9)	1455.9(10)
Z	4	2
D_{Calcd} (g cm^{-3})	1.438	1.623
μ (mm^{-1})	0.873	1.701
T (K)	293(2)	293(2)
λ (Mo-Kα) Å	0.71073	0.71073
Color	Green	Green
Shape	Block	Block
F(000)	1180	716
θ_{min}, θ_{max}(°)	3.09, 27.48	3.29, 27.77
$h_{min-max}$	$-12 \rightarrow 12$	$-7 \rightarrow 7$
$k_{min-max}$	$-22 \rightarrow 23$	$-13 \rightarrow 13$
$l_{min-max}$	$-19 \rightarrow 19$	$-28 \rightarrow 30$
R_{int}	0.0464	0.0626
No. unique data	5965	3304
No. of observed	4928	2316
No. variables	355	191
Completeness	99.7%	97.1%
$R_1[I > 2\sigma(I)]^a$	0.0346	0.0416
$wR_2[I > 2(I)]^b$	0.0811	0.0852
GOF	1.016	1.045
$(\Delta p)_{max,\ min}$ (e Å^{-3})	0.232, −0.355	0.468, −0.355
$(\Delta/\sigma)_{max,\ min}$	0.000, 0.000	0.001, 0.000
Flack parameter	0.00(4)	–

graphite-monochromated Mo-Kα radiation ($\lambda = 0.71073$ Å) and ω scan mode. The structures were solved by direct methods with SHELXS-97 [10] and refined by full-matrix least squares calculations with SHELXL-97 [11]. All non-hydrogen atoms in the two complexes were refined anisotropically. All hydrogens were located in calculated positions or found from different Fourier maps. Crystallographic data for **1** and **2** are listed in table 1. Selected bond lengths and angles of **1** and **2** are given in tables 2 and 3. Hydrogen bond distances and angles are listed in table 4.

3. Results and discussion

3.1. *Crystal structure*

3.1.1. CuL_2 (1). The crystal structure of **1** belongs to an acentric space group $Pna2_1$. As illustrated in figure 1, **1** consists of one Cu(II) and two deprotonated

Table 2. Selected bond lengths (Å) and angles (°) for **1**.

Cu(1)–N(1)	2.136(2)	Cu(1)–N(2)	1.899(2)
Cu(1)–N(4)	2.260(2)	Cu(1)–N(5)	1.931(2)
Cu(1)–O(2)	2.170(2)	Cu(1)–O(4)	2.355(2)
N(2)–Cu(1)–N(5)	176.90(10)	N(2)–Cu(1)–N(1)	77.94(9)
N(5)–Cu(1)–N(1)	102.39(9)	N(2)–Cu(1)–O(2)	77.96(8)
N(5)–Cu(1)–O(2)	101.72(8)	N(1)–Cu(1)–O(2)	155.88(7)
N(2)–Cu(1)–N(4)	106.97(9)	N(5)–Cu(1)–N(4)	76.13(8)
N(1)–Cu(1)–N(4)	87.09(9)	O(2)–Cu(1)–N(4)	99.01(8)
N(2)–Cu(1)–O(4)	102.00(8)	N(5)–Cu(1)–O(4)	74.90(7)
N(1)–Cu(1)–O(4)	98.66(8)	O(2)–Cu(1)–O(4)	87.28(7)
N(4)–Cu(1)–O(4)	151.03(6)		

Table 3. Selected bond lengths (Å) and angles (°) for **2**.

Cu(1)–N(1)	2.034(3)	Cu(1)–Cl(1)	2.208(1)
Cu(1)–N(2)	1.894(3)	Cu(1)–Cl(1A)	2.715(1)
Cu(1)–O(2)	2.047(2)		
N(2)–Cu(1)–N(1)	80.55(11)	N(2)–Cu(1)–O(2)	79.32(10)
N(1)–Cu(1)–O(2)	158.59(10)	N(2)–Cu(1)–Cl(1)	171.76(9)
N(1)–Cu(1)–Cl(1)	99.62(8)	O(2)–Cu(1)–Cl(1)	99.25(7)
N(2)–Cu(1)–Cl(1A)	98.56(9)	N(1)–Cu(1)–Cl(1A)	87.59(8)
O(2)–Cu(1)–Cl(1A)	102.56(8)	Cl(1)–Cu(1)–Cl(1A)	89.68(4)
Cu(1)–Cl(1)–Cu(1A)	90.32(4)		

Symmetry code A: $-x+1$, $-y$, $-z+1$.

Table 4. Hydrogen bond distances (Å) and angles (°) in **1** and **2**.

Complex	D–H···A	D–H	H···A	D···A	<DHA
1	N3–H3···O3#1	0.95	1.87	2.786(3)	162.4
	N6–H6···O4#2	0.88	2.15	3.011(2)	166.5
2	N3–H3A···O1#3	0.97	1.79	2.738(3)	162.5
	C5–H5A···Cl1#4	0.93	2.79	3.566(3)	141.7
	C8–H8B···Cl1#5	0.97	2.78	3.389(4)	121.7

Symmetry codes: #1: $1+x$, y, z; #2: $-1/2+x$, $1/2-y$, z; #3: $-x+2$, $-y+1$, $-z+1$, #4: $-x$, $-y$, $1-z$, #5: $1+x$, y, z.

picoloylhydrazide ligands L. The Cu(II) has a strongly distorted octahedral geometry with the equatorial plane defined by N(1), N(2), and O(2) atoms from one picoloylhydrazide ligand L and N(5) atom from the other picoloylhydrazide ligand L, while two remaining donors (N(4) and O(4)) of L occupy the axial sites. The Cu(1)–O(4) bond of 2.355(2) Å is 0.18 Å longer than Cu(1)–O(2) bond of 2.170(2) Å. The axial position is significantly bent due to the restriction imposed by the ligand geometry with the N(4)–Cu(1)–O(4) angle 151.03(6)°. The bond length of the Cu–$N_{pyridine}$ (Cu(1)–N(1) = 2.136(2), Cu(1)–N(4) = 2.260(2) Å) is longer than that of Cu–$N_{hydrazine}$ (Cu(1)–N(2) = 1.899(2), Cu(1)–N(5) = 1.931(2) Å), indicating that the former bond is

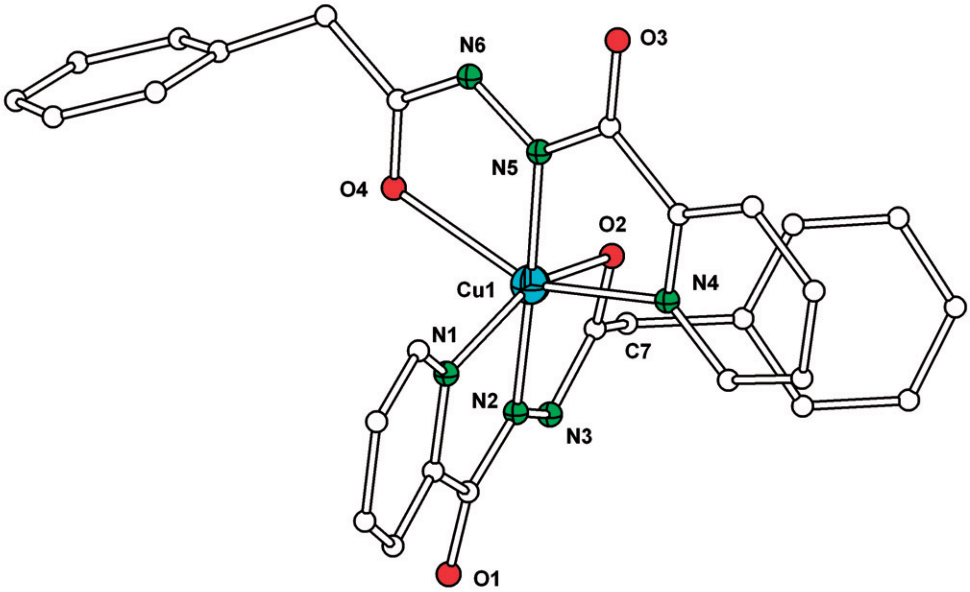

Figure 1. Structural representation of CuL_2 (**1**). Hydrogen atoms are omitted for clarity.

weaker than the latter [12, 13]. The two picoloylhydrazide ligands in **1** are non-coplanar, the dihedral angle between pyridine ring and benzene ring in the same ligand is 66.3 and 55.4°, respectively.

The hydrazine nitrogens and the acyl oxygens in two neighboring molecules link the discrete complexes to each other through the $N–H\cdots O$ hydrogen bonding interactions ($N3–H3\cdots O3\#1$ (#1 $1+x$, y, z), $N6–H6\cdots O4\#2$ (#2 $-1/2+x$, $1/2-y$, z)), forming a double-stranded chain along *a*. Neighboring chains are connected into an extended 2-D supramolecular structure through $\pi\cdots\pi$ interactions between neighboring pyridine rings (centroid–centroid distance 3.765 Å, interplanar distance 3.548 Å) and the $C–H\cdots\pi$ interactions between pyridyl hydrogen and the benzene ring of the neighboring molecule ($H\cdots$ centroid 2.86 and 2.54 Å, $C–H\cdots$ centroid angle 115 and 158°, respectively) (figure 2).

3.1.2. $Cu_2L_2Cl_2$ (2).

The coordination geometry of copper in **2** is a severely distorted square pyramid with a τ value of 0.22 (figure 3) [14]. Three donors of the tridentate ligand and one bridging chloride form the basal plane; the apical site is occupied by the other bridging chloride. Similar to **1**, the $Cu–N_{pyridine}$ bond length (2.034(3) Å) is longer than that of $Cu–N_{hydrazine}$ (1.894(3) Å). Each chloride bridges two Cu(II) ions in the equatorial-axial mode. The ligands are non-coplanar with the dihedral angle between pyridine and benzene being 66.9°, and they are disposed in a parallel manner with respect to one another.

Binuclear **2** with a $Cu_2(\mu\text{-}Cl)_2$ core has a crystallographic center of inversion. For the binuclear copper complexes with $Cu_2(\mu\text{-}Cl)_2$ core, there are two types of structures (planar structure and non-planar structure) [12, 15]. These structural differences in the complexes have substantial influences on frontier orbital compositions and

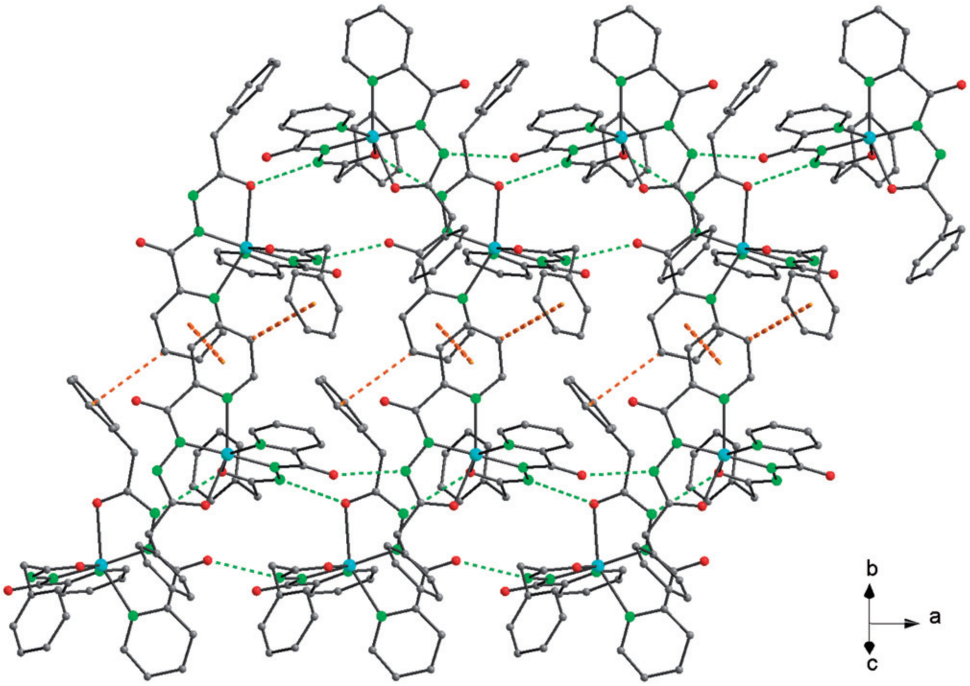

Figure 2. Extended 2-D structure of **1**. Hydrogen atoms are omitted for clarity.

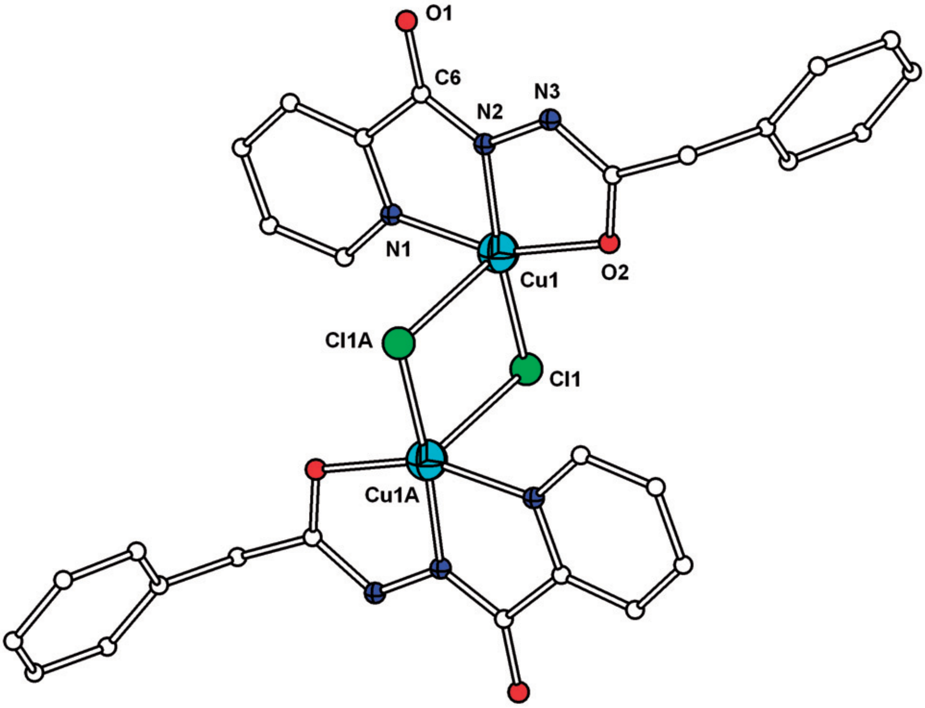

Figure 3. Structural representation of $Cu_2L_2Cl_2$ (**2**). Hydrogen atoms are omitted for clarity.

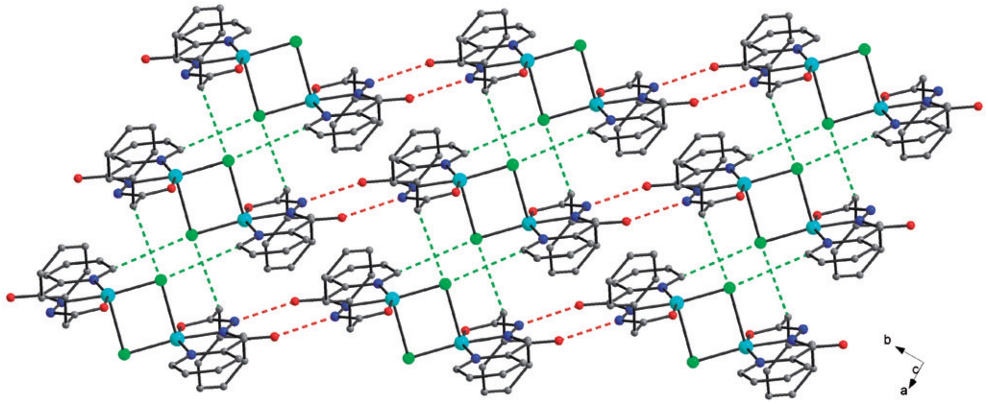

Figure 4. 2-D layer of **2** linked *via* hydrogen bonds. Hydrogen atoms are omitted for clarity.

energies and generate significant variations in their magnetic behavior [15]. The $Cu_2(\mu\text{-}Cl)_2$ core of **2** is perfectly planar, with rhomboidal geometry of two short Cu–Cl distances (Cu1–Cl1 2.208(1) Å) and two long Cu–Cl distances (Cu1–Cl1A 2.715(1) Å). The core bond angles are Cl1Cu1Cl1A 89.68(4)° and CuClCu1A 90.32(4)°. The Cu(1) $\cdots$ Cu(1A) distance is 3.509(1) Å, which indicates weak Cu $\cdots$ Cu interactions and can be compared to analogous binuclear copper complexes containing the $Cu_2(\mu\text{-}Cl)_2$ core [16–18].

The binuclear molecules extend to 1-D chains along the [1, 1, 0] direction through hydrogen bonds between the hydrazine nitrogens and acyl oxygens N3–H3A $\cdots$ O1#3 (symmetry code #3: $-x+1$, $-y$, $-z+1$). These 1-D chains further result in the formation of an infinite 2-D supramolecular layer along the *ab* plane through C–H $\cdots$ Cl interactions (figure 4).

3.2. *IR spectroscopic studies and fluorescence*

The HL shows that stretching bands attributed to N–H at 3226 cm^{-1} and to C=O at 1636 cm^{-1}. Absorptions at 1666 cm^{-1} for **1** and 1672 cm^{-1} for **2** are attributed to C=O stretching. The bands at 3472 for **1** and 3412 cm^{-1} for **2** can be attributed to N–H stretching. A series of bands observed in the range 3030–2800 cm^{-1} in the spectra of these compounds is assigned to the C–H stretches.

The pure ligand *N*-phenylacetyl picoloylhydrazide (HL) shows intense emission in solid state at 400 nm ($\lambda_{ex} = 250$ nm), and **1** and **2** have similar emissions at 396 nm and 400 nm ($\lambda_{ex} = 250$ nm) (figure 5). Both excitation and emission wavelengths of the title complexes are similar to that of the free ligand. Therefore, the emission of the pure ligand and **1** and **2** are attributed to the $\pi \rightarrow \pi^*$ transition [19, 20].

3.3. *Magnetic properties*

3.3.1. CuL_2 (1). The variable-temperature (2–300 K) magnetic susceptibility of **1** has been measured on a crystalline sample under an applied magnetic field of 1 T. The plots of χ_M and $\chi_M T$ *versus* T of **1** are shown in figure 6, where χ_M is the magnetic

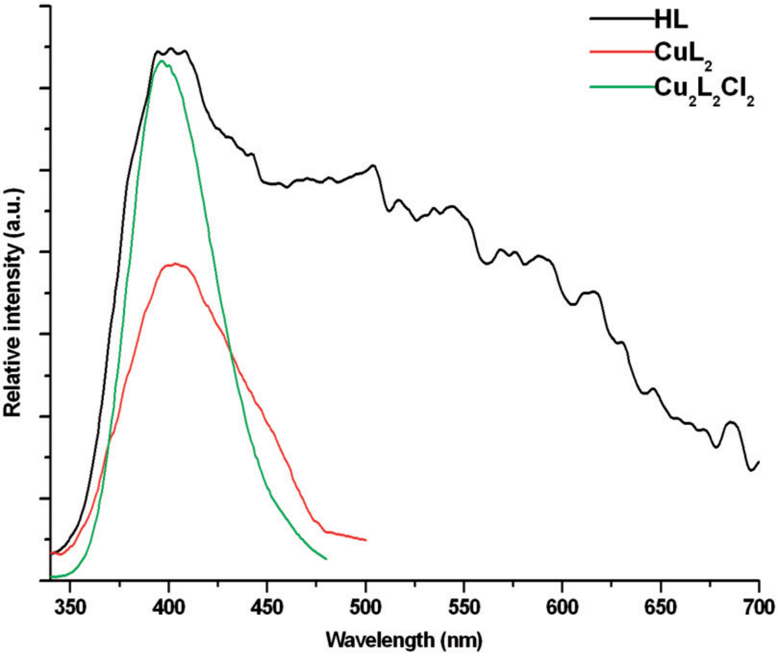

Figure 5. The emission spectra of **1**, **2**, and HL in solid state at room temperature.

susceptibility per Cu^{II} unit. The $\chi_M T$ per Cu^{II} unit at 300 K is equal to $0.53\,cm^3\,mol^{-1}\,K$, slightly larger than the expected value of $0.37\,cm^3\,mol^{-1}\,K$ for one isolated Cu^{II} unit. As the temperature is lowered, the $\chi_M T$ decreases more and more rapidly to $0.27\,cm^3\,mol^{-1}\,K$ at 10 K and then decreases abruptly to $0.20\,cm^3\,mol^{-1}\,K$ at 2 K. A nonlinear fit in the temperature range of 50–300 K reveals a Curie–Weiss behavior with a Curie constant, C, of $0.38\,cm^3\,mol^{-1}\,K$ and a Weiss constant, θ, of -8.27 K, suggesting weak intermolecular antiferromagnetic interaction between the copper(II) centers.

The field dependence of the magnetization for **1** was measured at 2 K (figure S2). The magnetization first increases abruptly with increased field and then slowly. The *M versus H* curve shows that the magnetization is still not saturated up to 8 T with a value of *ca* 0.08 Nβ.

3.3.2. $Cu_2L_2Cl_2$ (2).

The plots of χ_M and $\chi_M T$ *versus* T of **2** are shown in figure 7, where χ_M is the magnetic susceptibility per Cu^{II} unit. The $\chi_M T$ per Cu^{II} unit at 300 K is $1.01\,cm^3\,mol^{-1}\,K$. Upon cooling, the $\chi_M T$ decreases continuously to a value of $0.57\,cm^3\,mol^{-1}\,K$ at 12 K, followed by an abrupt decrease to $0.14\,cm^3\,mol^{-1}\,K$ at 2 K. A nonlinear fit in the temperature range of 50–300 K reveals a Curie–Weiss behavior with a Curie constant, C, of $0.77\,cm^3\,mol^{-1}\,K$ and a Weiss constant, θ, of -15.1 K. This behavior is due to antiferromagnetic coupling between copper(II) centers.

The field dependence of the magnetization for **2** was measured at 2 K (figure S3). The magnetization first increases slowly with increased field and then increases

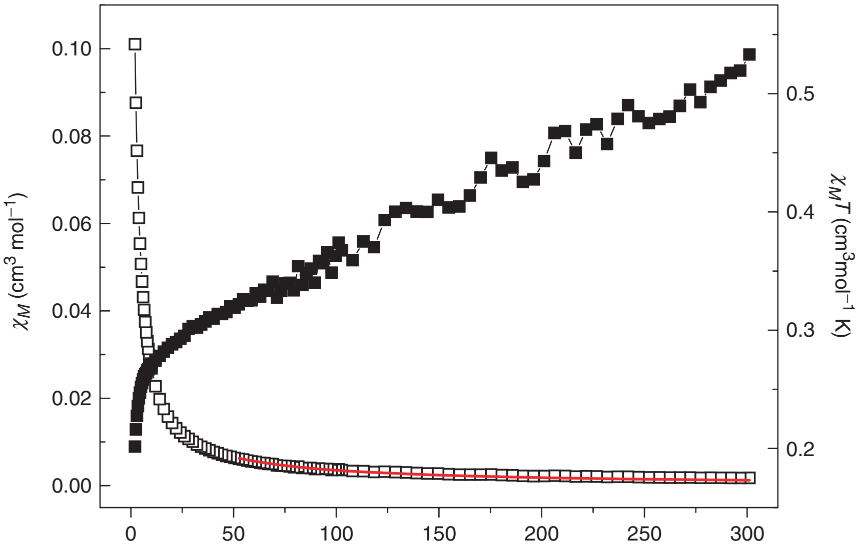

Figure 6. Temperature dependence of χ_M and $\chi_M T$ for **1** with the solid line showing the best fit.

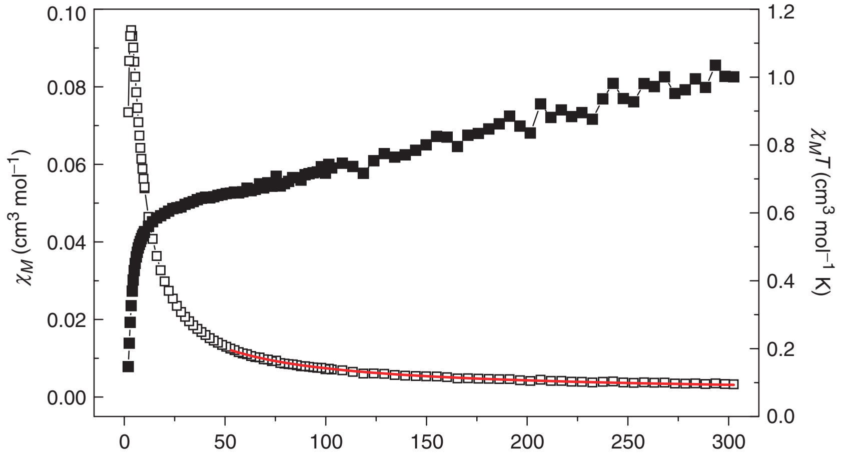

Figure 7. Temperature dependence of χ_M and $\chi_M T$ for **2** with the solid line showing the best fit.

fast, followed by another slow increase, forming an S-shaped curve. The *M versus H* curve shows that the magnetization is still not saturated up to 8 T with a value of *ca* 0.12 Nβ.

4. Conclusions

The preparation, crystal structures and characterization of two copper(II) complexes with *N*-phenylacetyl picoloylhydrazide (HL) have been reported. The complex CuL_2 (**1**) and binuclear complex $Cu_2Cl_2L_2$ with a $Cu_2(\mu\text{-Cl})_2$ core (**2**) were synthesized from

$Cu(OAc)_2 \cdot H_2O$ or $CuCl_2 \cdot 2H_2O$. Neighboring molecules are connected into 2-D supramolecular structures through non-covalent intermolecular bonds. Non-covalent intermolecular bonds play an important role in the architecture of supramolecular structure and increase of crystal structure stability.

Supplementary material

The crystallographic data of the structures described in this article were deposited in the Cambridge Crystallographic Data Center with the CCDC deposition numbers 681326 and 681327, respectively. The IR spectra curves for ligand HL and the two title complexes and the *M versus H* curves for **1** and **2** were deposited in the online version.

Acknowledgments

This project was financially supported by the Natural Science Foundation of China (Nos. 20431010 and 20171012) and the Natural Science Foundation of Fujian Province, China (E0110010).

References

[1] L.K. Thompson. *Coord. Chem. Rev.*, **233**, 193 (2002).
[2] E.Q. Gao, S.Q. Bai, Z.M. Wang, C.H. Yan. *J. Am. Chem. Soc.*, **125**, 4984 (2003).
[3] C.J. Matthews, K. Avery, Z. Xu, L.K. Thompson, L. Zhao, D.O. Miller, K. Biradha, K. Poirier, M.J. Zaworotko, C. Wilson, A.E. Goeta, J.A.K. Howard. *Inorg. Chem.*, **38**, 5266 (1999).
[4] J. Cano, G.D. Munno, F. Lloret, M. Julve. *Inorg. Chem.*, **39**, 1611 (2000).
[5] S. Lin, S.X. Liu, J.Q. Huang, C.C. Lin. *J. Chem. Soc., Dalton Trans.*, 1595 (2002).
[6] Y.F. Yue, E.Q. Gao, C.J. Fang, S. Xu, C.H. Yan. *J. Mol. Struct.*, **841**, 67 (2007).
[7] L. Pan, X. Huang, J. Li, Y. Wu, N. Zheng. *Angew. Chem. Int. Ed.*, **39**, 527 (2000).
[8] X. Xu, Y. Ma, Y. Lu, E. Wang, X. Bai. *J. Mol. Struct.*, **828**, 68 (2007).
[9] Z.D. Tomić, V.M. Leovac, S.V. Pokorni, D. Zobel, S.D. Zarić. *Eur. J. Inorg. Chem.*, 1222 (2003).
[10] G.M. Sheldrick. *SHELXS-97, Program for X-ray Crystal Structure Solution*, University of Gőttingen, Gőttingen, Germany (1997).
[11] G.M. Sheldrick. *SHELXS-97, Program for X-ray Crystal Structure Refinement*, University of Gőttingen, Gőttingen, Germany (1997).
[12] P.F. Rapheal, E. Manoj, M.R.P. Kurup. *Polyhedron*, **26**, 818 (2007).
[13] V. Philip, V. Suni, M.R.P. Kurup, M. Nethaji. *Polyhedron*, **24**, 1133 (2005).
[14] A.W. Addison, T.N. Rao, J. Reedijk, J. van Rijn, G.C. Verschoor. *J. Chem. Soc., Dalton Trans.*, 1349 (1984).
[15] P. Kapoor, A. Pathak, R. Kapoor, P. Venugopalan. *Inorg. Chem.*, **41**, 6153 (2002).
[16] M. Rodríguez, A. Llobet. *Inorg. Chem.*, **38**, 2328 (1999).
[17] E. Colacio, M. Ghazi, R. Kivekäs, J.M. Moreno. *Inorg. Chem.*, **39**, 2882 (2000).
[18] M.E. Bluhm, M. Ciesielski, H. Gö1rls, O. Walter, M. Dö1ring. *Inorg. Chem.*, **42**, 8878 (2003).
[19] Z.F. Chen, R.G. Xiong, J. Zhang, X.T. Chen, Z.L. Xue, X.Z. You. *Inorg. Chem.*, **40**, 4075 (2001).
[20] L.L. Wen, D.B. Dang, C.Y. Duan, Y.Z. Li, Z.F. Tian, Q.J. Meng. *Inorg. Chem.*, **44**, 7161 (2005).